Methane distribution in European tidal estuaries

JACK J. MIDDELBURG[1], JOOP NIEUWENHUIZE[1], NIELS IVERSEN[2], NANA HØGH[2], HEIN DE WILDE[3,*], WIM HELDER[3], RICHARD SEIFERT[4] & OLIVER CHRISTOF[4]

[1]*Netherlands Institute of Ecology, Korringaweg 7, 4401 NT Yerseke, The Netherlands (E-mail: middelburg@cemo.nioo.knaw.nl);* [2]*Aalborg University, Department of Civil Engineering, Environmental Engineering Laboratory, Sohngaardsholmvej 57, 9000 Aalborg, Denmark;* [3]*Netherlands Institute of Sea Research, Postbus 59, 1790 AB Den Burg, The Netherlands;* [4]*Institute of Biogeochemistry and Marine Chemistry, University of Hamburg, Bundesstrasse 55, 20146 Hamburg, Germany (*Present address: ECN, Postbus 1, 1755 ZG Petten, The Netherlands)*

Abstract. Methane concentrations have been measured along salinity profiles in nine tidal estuaries in Europe (Elbe, Ems, Thames, Rhine, Scheldt, Loire, Gironde, Douro and Sado). The Rhine, Scheldt and Gironde estuaries have been studied seasonally. A number of different methodologies have been used and they yielded consistent results. Surface water concentrations ranged from 0.002 to 3.6 μM, corresponding to saturation ratios of 0.7 to 1580 with a median of 25. Methane concentrations in the fresh-water end-members varied from 0.01 to 1.4 μM. Methane concentrations in the marine end-members were close to saturation offshore and on the order of 0.1 μM in estuarine plumes. Methane versus salinity profiles in river-dominated, stratified estuaries (Rhine and Douro) appeared rather erratic whereas those in the well mixed, long-residence time estuaries (Elbe, Ems, Thames, Scheldt, Loire, Gironde and Sado) revealed consistent trends. In these systems dissolved methane initially decreases with increasing salinity, then increases to a maximum at intermediate to high salinities before decreasing again going offshore. Tidal flats and creeks were identified as a methane source to estuarine waters. The global estuarine flux of methane to the atmosphere has been calculated by combining the median water-air methane gradient (68.2 nmol dm^{-3}) with a global area weighted transfer coefficient and the global area of estuaries. Estuaries emit 1.1 to 3.0 Tg CH$_4$ yr^{-1}, which is less than 9% of the global marine methane emission.

Introduction

Methane is an atmospheric trace gas that contributes significantly to the greenhouse effect (15%) and is involved in a number of chemical reactions (Cicerone & Oremland 1988). Global atmospheric methane concentration has

been increasing over the last two centuries indicating that methane sources are larger than methane sinks. This increase in methane will affect the radiative and chemical balance of the atmosphere. Consequently, scientists have extended much effort in identifying and quantifying source and sinks terms in the global methane budget. There is consensus in the literature that the marine environment represents a small source of methane to the atmosphere (5 to 50 Tg or between 1 and 10% of total methane emission; Cicerone & Oremland 1988; Bange et al. 1994; Prather et al. 1995). Although shelf and estuaries represent only about 15.2 and 0.4% of the global ocean area respectively, they account for about 68 and 7.4% of the oceanic emission, respectively (Bange et al. 1994). However, these estimates for the coastal environment are rather uncertain due to high spatial and temporal variability and the limited data available.

Dissolved methane concentrations in open ocean waters are usually slightly saturated or close to saturation (about 2 to 3 nM), whereas those in the coastal zone can be orders of magnitude higher (e.g., De Angelis & Lilley 1987; Bugna et al. 1996; Scranton & McShane 1991; Watanabe et al. 1994; Bange et al. 1994, 1996, 1998; Sansone et al. 1998, 1999; Rehder et al. 1998; Seifert et al. 1999; Amouroux et al. 2002). Sources of methane include riverine inputs (Scranton & McShane 1991), diffusion from sediments (Hovland et al. 1993), methane production in microenvironments (De Angelis & Lee 1994), leakage from oil or gas production (Rehder et al. 1998) and submarine groundwater discharge (Bugna et al. 1996).

Rivers have dissolved methane concentrations one to two orders of magnitude higher than open ocean waters and riverine methane can be traced over long distances (Scranton & McShane 1991; Jones & Amador 1993). The distribution of methane in some estuaries is largely governed by riverine inputs and conservative mixing (e.g., De Angelis & Lilley 1987), while non-conservative behaviour due to methane outgassing, oxidation and estuarine sources has been identified in some other estuaries (e.g., Sansone et al. 1999). However, most studies either incompletely covered the estuarine salinity range or are based on few samples with the result that potential estuarine sinks and sources could not adequately be traced.

In this paper we present the distribution of methane in nine tidal estuaries along the European Atlantic coast (Elbe, Ems, Thames, Rhine, Scheldt, Loire, Gironde, Douro and Sado). The entire salinity range was covered with a resolution of 2 to 3 units so that conservative behaviour and estuarine sources and sinks could be evaluated. Moreover, the Rhine, Scheldt and Gironde estuaries were studied four times to reveal seasonal variability and the upper part of the Scheldt estuary was studied at monthly resolution to better constrain seasonality. This large-scale survey involved four laboratories

Figure 1. Geographic locations of investigated estuaries.

employing different sampling and analytical procedures. There was overlap in the data so that comparisons between sampling and analytical protocols could be made.

Study areas

The estuaries investigated are situated along the European Atlantic coast and cover a North-South gradient (Figure 1). Some basic characteristics of the estuaries are summarised in Table 1. The biogeochemical processes and trace gas distribution in these estuaries have been studied during the project BIOgas transfer in ESTuaries (BIOGEST); an overview of the project is given by Frankignoulle & Middelburg (2002).

Table 1. Overview of estuaries and cruises

Cruise	Date (cruise number)	Area (km^2)	Drainage basin (10^3 km^2)	Water residence (d)	Tidal flats[1]
Elbe	April 1997 (1)	327	146	15–30	+
Ems	July 1997 (2)	162	13	14–70	+ + +
Thames	February 1999 (3)	215	14	30	+
Rhine	October 1996 (4), July 1997 (5)	71	224	2–7	–
	November 1997 (6), April 1998 (7)				
Scheldt	June 1996 (8), December 1996 (9)	269	22	30–90	++
	May 1998 (10), October 1998 (11)				
	April 1997 to April 1998 (12)				
Loire	September 1998 (13)	41	121	30	+
Gironde	October 1996 (14), June 1997 (15)	442	85	30–90	+
	September 1997 (16), February 1998 (17)				
Douro	September 1998 (18)	2	115	2–7	+
Sado	September 1998(19)	102	8	30	+ + +

[1] The number of crosses indicates the relative importance of tidal flats.

The river Elbe, which drains northeastern Germany and the northern part of the Czech republic, feeds the Elbe estuary, a well-mixed estuary with a long residence time. The Ems estuary (the Netherlands, Germany) connects the northeastern part of the Netherlands and the northwestern part of Germany with the North Sea. It is a typical well-mixed tidal estuary with long residence times and high suspended matter (SPM) concentrations. There are large inter-tidal flats in the lower (the Wadden Sea) and middle reaches (Dollard) that cover about 50% of the total surface area. The Thames estuary is a turbid, tidal estuary on the east coast of the United Kingdom, entering the North Sea at Southend on Sea. The drainage area of the river Thames is rather small (14000 km^2) but hosts a population of about 12 million, including London. The drainage basin of the river Rhine covers large areas of Switzer-land, Germany and the Netherlands and smaller areas of Austria, France, Luxembourg and Belgium. The major part of Rhine water is discharged into the North Sea through the Nieuwe Waterweg, a typical river-dominated, salt-wedge estuary with a short water residence time and no tidal flats. The river Scheldt, which drains western Belgium and parts of Northwest France and Southwest Netherlands, feeds the Scheldt estuary, a well-mixed estuary with a long water residence time. The river Loire drains a major part of central France and its estuary is well-mixed and very turbid with SPM concentrations over 1 g l^{-1}. The rivers Garonne and Dordogne that drain a large part of southwestern France feed the Gironde estuary, which is a well-mixed, highly

turbid estuary with SPM concentrations over 1 g l^{-1}. The river Douro drains large areas of northern Portugal and Spain before it flows into the Atlantic Ocean near the city of Porto and is a typical salt-wedge type estuary with a short water residence time. The river Sado drains the southern part of Portugal and its estuary is well mixed with large intertidal areas (Maratera).

Basically, the Douro and Rhine estuaries are typical salt-wedge estuaries with short water residence time and low turbidity, whereas the others are vertically and laterally well-mixed, turbid and have long water residence times. The Ems, Scheldt, Thames, Loire and Sado estuaries are highly hetero-trophic with high partial pressures of carbon dioxide, high carbon dioxide effluxes and low oxygen concentrations, while the Elbe and Rhine estuaries are well oxygenated and have relatively low partial pressures of carbon dioxide (Frankignoulle et al. 1998).

Sampling and analysis

Dissolved methane concentrations have been quantified using five approaches (Table 2). Three of them involved taking surface samples (upper 1 meter) using a 20 litre Niskin bottle and sequential subsampling. These discrete samples were taken along the spine of the estuaries at salinity intervals of 2 to 3 units during campaigns typically lasting 3 to 5 days. Some additional samples were taken using a Zodiac to trace the effect of tidal flats and creeks on methane concentrations. The other two methods involved pumping of seawater from depths more than 1 meter into an equilibrator. This differ-ence in sampling depths between discrete and equilibrator methods may have consequences for methane results in stratified systems such as the Rhine and Douro estuaries. The reproducibility of all five methods is about 5% or better (2%: equilibrator-GC-FID). Gas concentrations have been quantified using working or commercial (Hoekloos, Linde) standards traceable to NIST-USA or NOAA standards and they were internally consistent.

The GC-FID-storage method involves collecting subsamples without headspace in 55-ml vials capped with Teflon-lined butyl rubber septa. Before upside down storage and transport to the home laboratory, nitrogen filled headspace of 5 ml was created and 100 μl concentrated sulphuric acid was added. Test experiments showed that storage after addition of sulphuric acid or $HgCl_2$ resulted in negligible loss. Methane in the headspace was measured using a Carlo Erba MEGA 5340 Gas Chromatograph (GC) equipped with a (2 m × 2 mm) Haysep column and a Flame Ionisation Detector (FID).

The GC-FID method was very similar, except that 160 ml glass serum bottles with butyl rubber septa were used, a 50 ml nitrogen headspace was created immediately after sampling and that measurements were made

Table 2. Overview of methodologies

Sampling	Partitioning	Quantification	Cruises covered
Discrete	Headspace	GC-FID-storage	1–8, 13–16, 18
Discrete	Headspace	GC-FID	2, 3, 5, 8–11, 13–17, 19
Discrete	Purge-trapping	GC-FID	1, 9, 11, 15, 16
Pumping	Equilibrator	GC-FID	2, 4–7, 15, 16
Pumping	Equilibrator	Photo-acoustic-IR	2–8, 12–16, 18

onboard ship after a few hours of shaking using a Chrompack 438 GC with a (2 m × 2 mm) Haysep column and a FID.

Michaelis et al. (1990) and Seifert et al. (1999) have described the purge-trapping method. Briefly, subsamples of 600 ml were stripped for 30 minutes with a helium flow of 40-ml min^{-1}. The two-step trapping mechanism was maintained at $-80\,^{\circ}C$ with acetone and consisted of (1) an activated Al_2O_3 trap for all hydrocarbons but methane and (2) an activated charcoal trap for methane. The trapped hydrocarbons were released by stepwise heating to $90\,^{\circ}C$ and were quantified using a Carlo Erba 4200 GC with an activated Al_2O_3 column (3 m × 4 mm) and a FID. The non-methane hydrocarbon results will be presented elsewhere.

De Wilde and Helder (1997) have described the on-line equilibrator-GC-FID method in detail. During sailing seawater was continuously pumped and sprayed through a headspace of air in an equilibrator. The 95% response time of the equilibrator was about 5 minutes. The methane concentration in the equilibrator headspace relates directly to dissolved methane via the temperature and salinity dependent solubility function (Wiesenburg & Guinasso 1971). The methane in equilibrator headspace was quantified using a Chrompack CP9000 GC with a Haysep (3.5 m × 2.1 mm) column and a FID.

The equilibrator-IR method is very similar to the other equilibrator technique, except that the 95% response time was slower (about 20 minutes) because of lower water flow rates and that methane in the headspace of the equilibrator was quantified using a photo-acoustic Infrared detector (Bruel & Kjær 1302; Middelburg et al. 1996). This photo-acoustic detector allows on-line monitoring of carbon dioxide, nitrous oxide and methane with a resolution of 2 minutes. The average of >5 measurements at each station is used except for two cruises (November 1997 Rhine and December 1996 Scheldt) for which individual underway data are presented.

Quality control and data presentation

A direct comparison between the methods based on discrete samples is simple, whereas a comparison of these techniques with the equilibrator approaches is complicated because water being pumped into the equilibrator may differ in origin and salinity. Moreover, for logistic reasons the equilibrator-GC-FID method was sometimes installed on another ship than the one used for discrete sampling.

Figure 2(A) shows that the results obtained with the GC-FID-storage and GC-FID approaches are internally highly consistent ($r^2 = 0.98$, $N = 114$) with the geometric regression line not being significant different from one. These two approaches together covered all estuaries (Table 2). Agreement of the two static headspace based techniques (GC-FIC-storage and GC-FID) with the purge trapping technique is good ($r^2 = 0.77$, $N = 47$ and $r^2 = 0.81$, $N = 47$, respectively), in particular at concentrations below 0.2 μM ($r^2 = 0.94$, $N = 35$ and $r^2 = 0.87$, $N = 41$, respectively; Figure 2(C) and 2(D)). Figure 2(B) shows that the equilibrator-IR and GC-FID-storage technique are also internally consistent ($r^2 = 0.90$, $N = 178$), though there is substantial scatter. It should be realised that discrete samples reflect snapshot measurements of surface water, whereas equilibrator data give an integrative, delayed average over more than 20 minutes for subsurface water.

All dissolved methane data based on the GC-FID and GC-FID-storage methodologies and methane concentrations based on purge-trapping technique that were below 0.2 μM have been considered internally consistent and are presented as an average with standard deviations in Figures 3 to 6. This mode of presentation enhanced the clarity of methane versus salinity plots while all essential information was retained. In fact, standard deviations are often so small that error bars are hidden within the symbols. Equilibrator-IR data are presented for the complete annual cycle in the upper Scheldt estuary (Figure 8), for the November 1997 cruise in the Rhine (Figure 7) and for the December 1996 cruise in the Scheldt (Figure 5). The equilibrator-GC-FID data are presented as separate data for the Ems, July and September 1997 Gironde and the Rhine cruises (Figures 3, 4, 6).

Results

Dissolved methane concentrations are shown as a function of salinity in Figures 3 to 6. Dissolved methane concentrations ranged from 0.0021 to 3.6 μM and are all, except for one sample in the October 1996 Gironde cruise, above atmospheric equilibrium levels (0.002 to 0.003 μM). The equilibrium levels were calculated from temperature and salinity using the solubility data
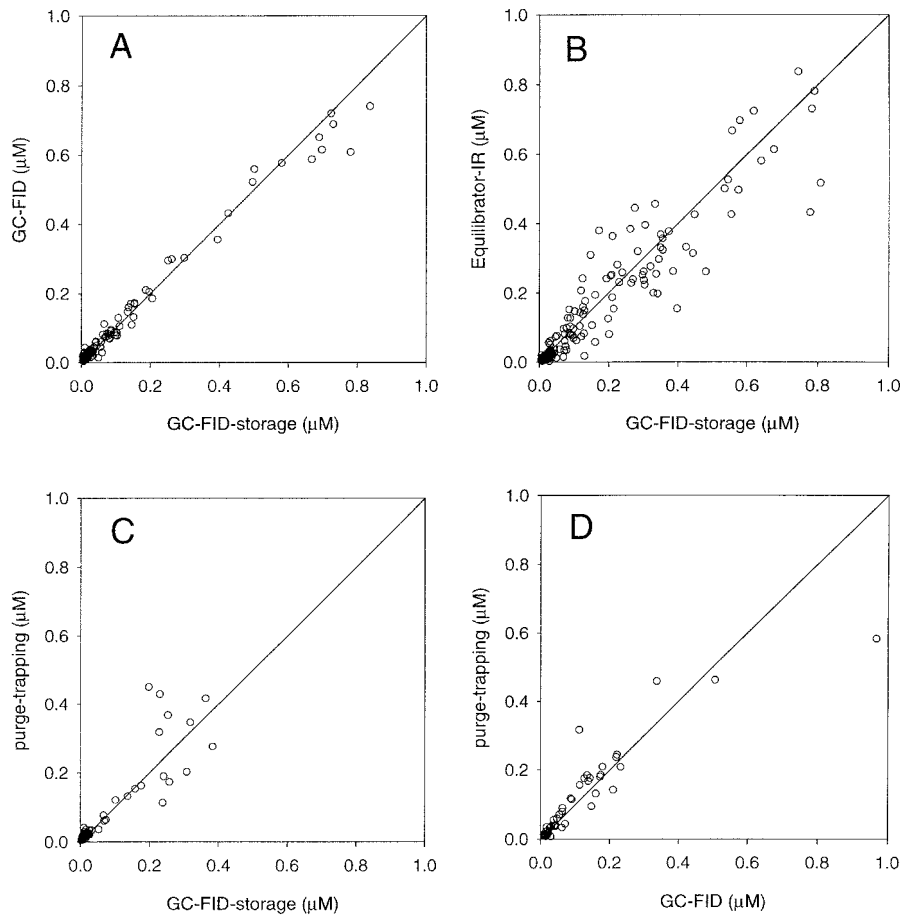
Figure 2. A: Methane concentration based on GC-FID versus GC-FID after storage. B: Methane concentration based on Equilibrator-Photo-acoustic IR detection versus GC-FID after storage. C: Methane concentration based on purge-trapping versus GC-FID after storage. D: Methane concentration based on purge-trapping versus GC-FID. Solid lines represent the 1:1 relationships.

of Wiesenburg and Guinasso (1979) and relative to an atmospheric methane mixing ratio of 1.9 ppmv (Bange et al., 1994). Atmospheric mixing ratios varied from 1.73 to >2.4 ppmv. Saturation ratios (observed methane divided by equilibrium concentration) ranged from 0.7 to 1580 with a median of 25 (Table 3).

Concentrations of methane in the rivers (fresh-water end-members) varied from 0.01 to 1.4 μM (Table 4). Marine end-member concentrations are based on the most saline samples collected and ranged from about 0.004 μM offshore in the North Sea (Rhine, Elbe and Thames cruises) to 0.1 μM

in the plumes of the Scheldt and Rhine estuaries (Table 4). Under steady state conditions conservative mixing between river and seawater would yield straight lines connecting the riverine and marine end-members. Figures 3 to 6 clearly show that conservative mixing was not occurring in any of the estuaries investigated.

The Elbe and Thames estuaries have high riverine concentrations (0.111 and 0.273 μM, respectively) and their methane versus salinity plots (Figure 3(A) and 3(C)) suggest that methane was consumed by oxidation and/or was lost to the atmosphere during transit through the estuary.

Methane versus salinity plots for the Ems (Figure 3(B)), Loire (Figure 3(D)), Sado (Figure 3(F)), Gironde (Figure 4) and Scheldt (Figure 5) estuaries clearly show that there were estuarine sinks due to oxidation and/or outgassing and estuarine sources. These estuarine sources were consistently observed as maxima at salinities 25 to 30 in the Scheldt estuary during the four seasons (Figure 5) and as maxima around salinity 20 in the Gironde estuary during summer and fall (Figure 4). Moreover, a few samples were collected above tidal flats or in tidal creeks to trace the source/sink term of tidal sediments. These samples were highly enriched in methane in the Dollard zone of the Ems estuary (Figure 3(B)), the Marteca area of the Sado estuary (Figure 3(F)) and the Gironde estuary (Figure 4, September).

The lowest methane concentrations in the Ems, Loire and Gironde estuaries were not only observed near the marine end-member, as in most estuaries, but also in the high turbidity zones at salinities 1 to 10 (Figures 3(B), 3(D) and 4). These low methane concentrations in the high turbidity zones of the Ems, Loire and Gironde estuaries may be due either to enhanced outgassing caused by high current velocities and turbulence levels or to enhanced methane oxidation by bacteria attached to these particles. The Loire and Gironde estuaries have layers of fluidised mud in which bacterial activity is enhanced relative to the water column above (Abril et al. 1999, 2000).

Methane versus salinity plots for the Douro (Figure 3(E)) and Rhine estuary (Figure 6) are rather scattered and do not allow us to extract methane sources or sinks. These estuaries have short water residence times (Table 1), show salinity stratification, and our sampling procedure based on a well-mixed water column may perhaps not have been appropriate. However, these scatter methane versus salinity plots were also obtained by the equilibrator-GD-FID approach (Figure 6) which has a higher reproducibility (about 2%) and gave rather smooth profiles in the Ems (Figure 3(B)) and the Gironde estuary (Figure 4). The observed variability is significantly higher than the standard error of the analysis suggesting that this variability is real and not an artefact of our sampling procedure.
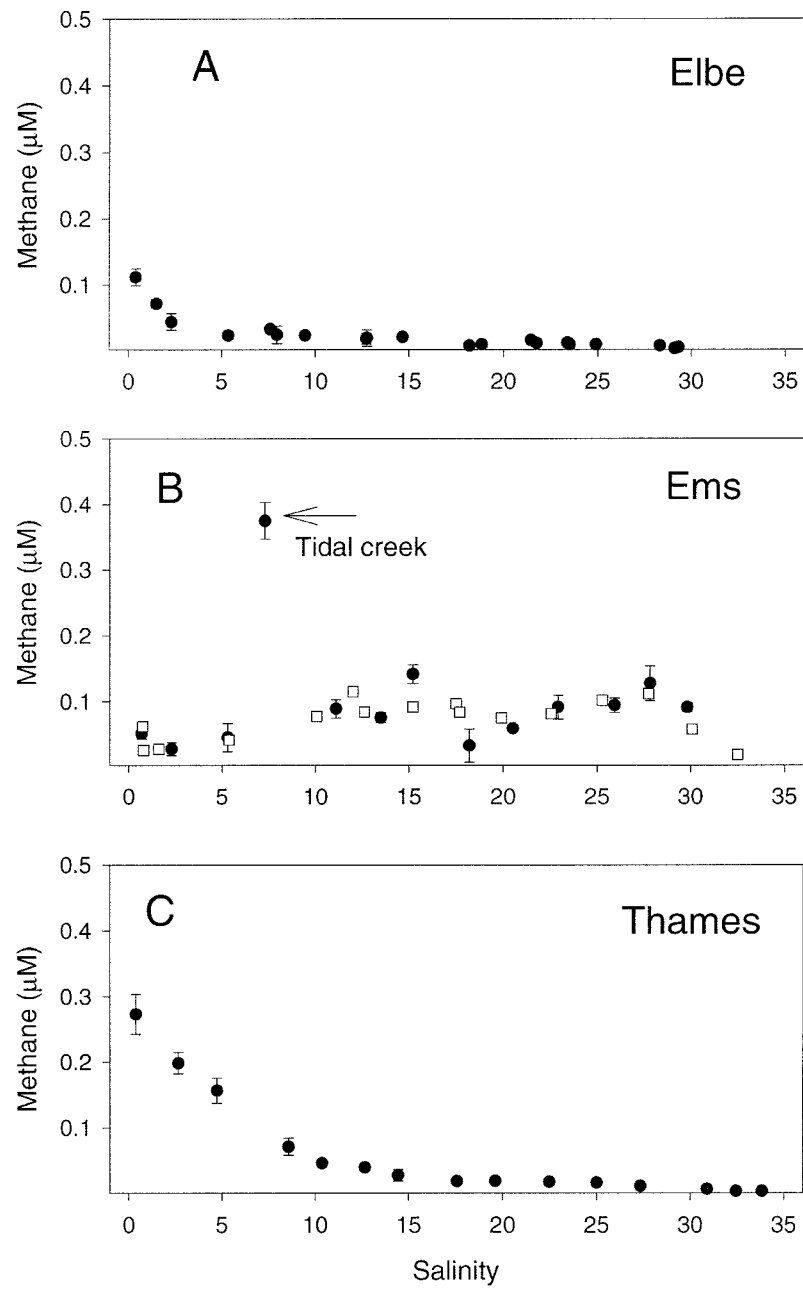
Figure 3. Dissolved methane versus salinity. A: Elbe estuary; B: Ems estuary; C: Thames estuary; D: Loire estuary; E: Douro estuary; F: Sado estuary. Solid symbols: average ± standard deviation of discrete samples; Open squares: equilibrator-GC-FID data. Notice the difference and breaks in methane concentration scale for the Loire and Sado estuaries. Arrows indicate samples collected in tidal creeks (Ems and Sado).
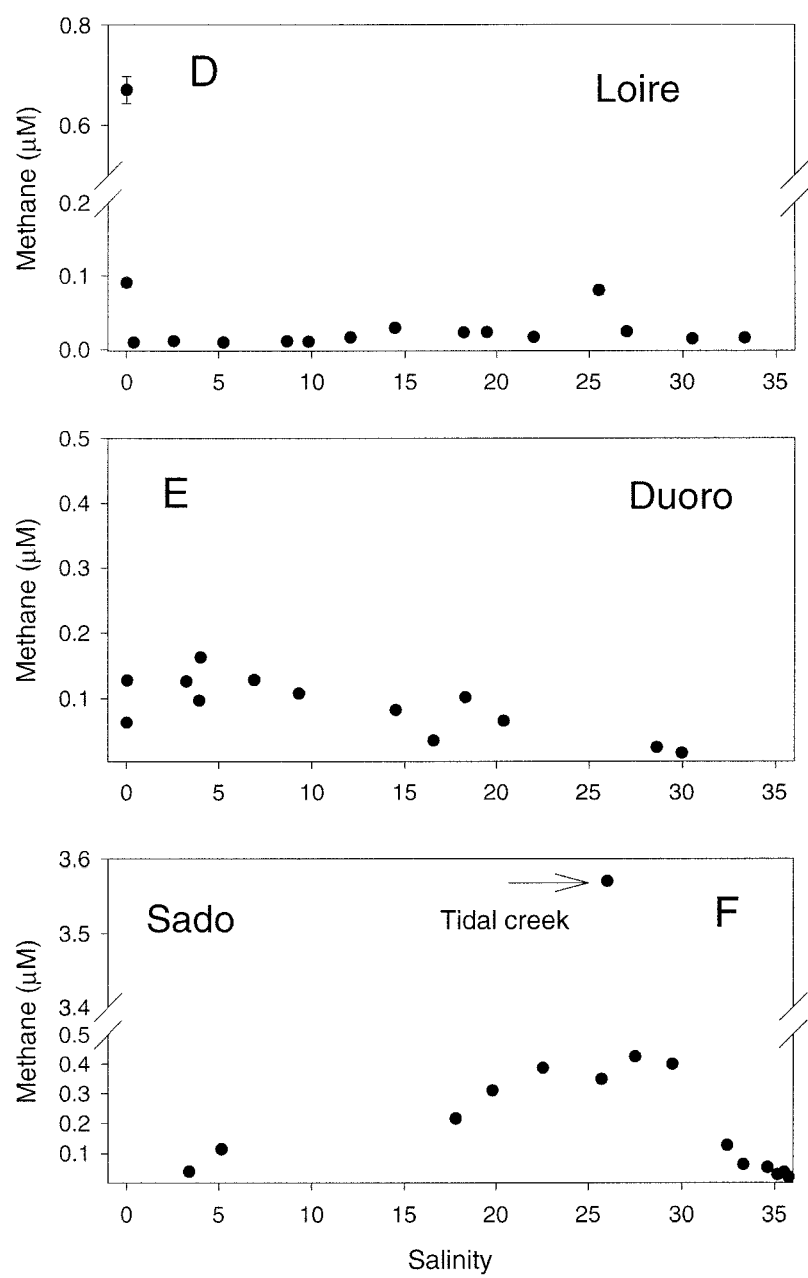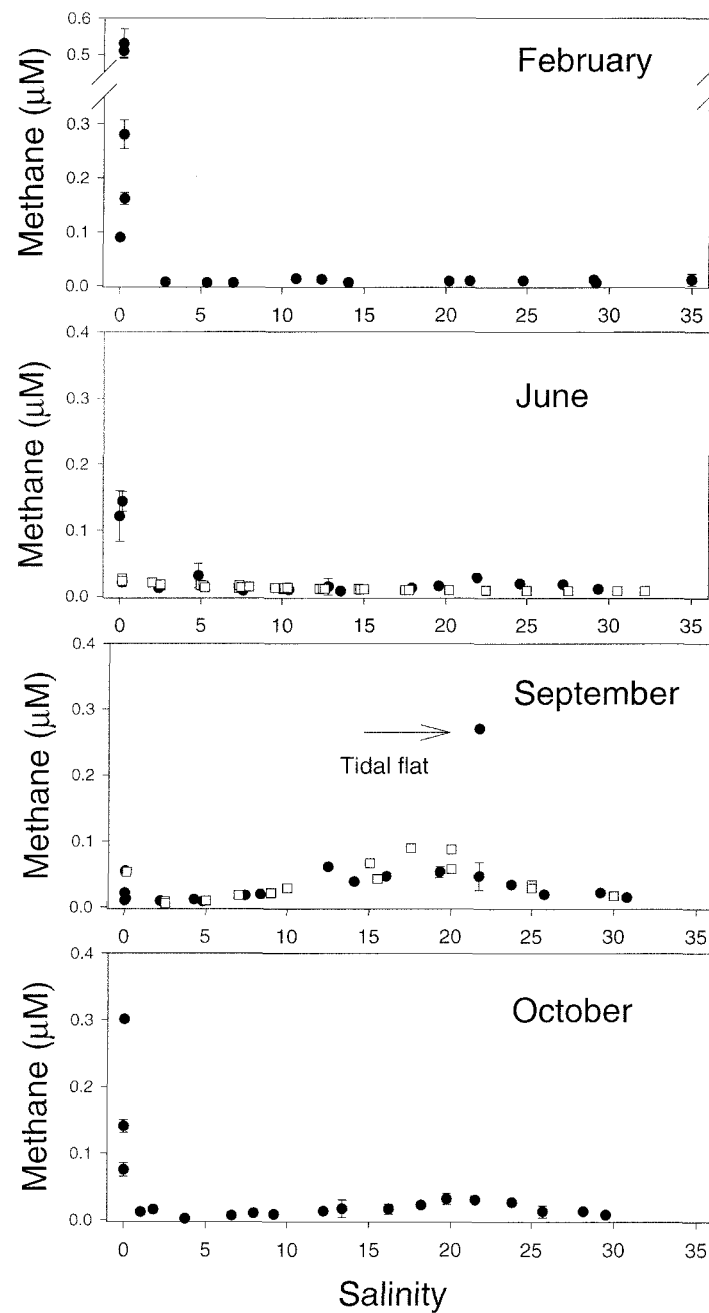
Figure 3. Continued.

Figure 4. Dissolved methane versus salinity in the Gironde estuary. Solid symbols: average ± standard deviation of discrete samples; Open squares: equilibrator-GC-FID data. Notice the difference and break in methane concentration scale for February 1998. Arrow indicates samples collected above tidal flat (September).
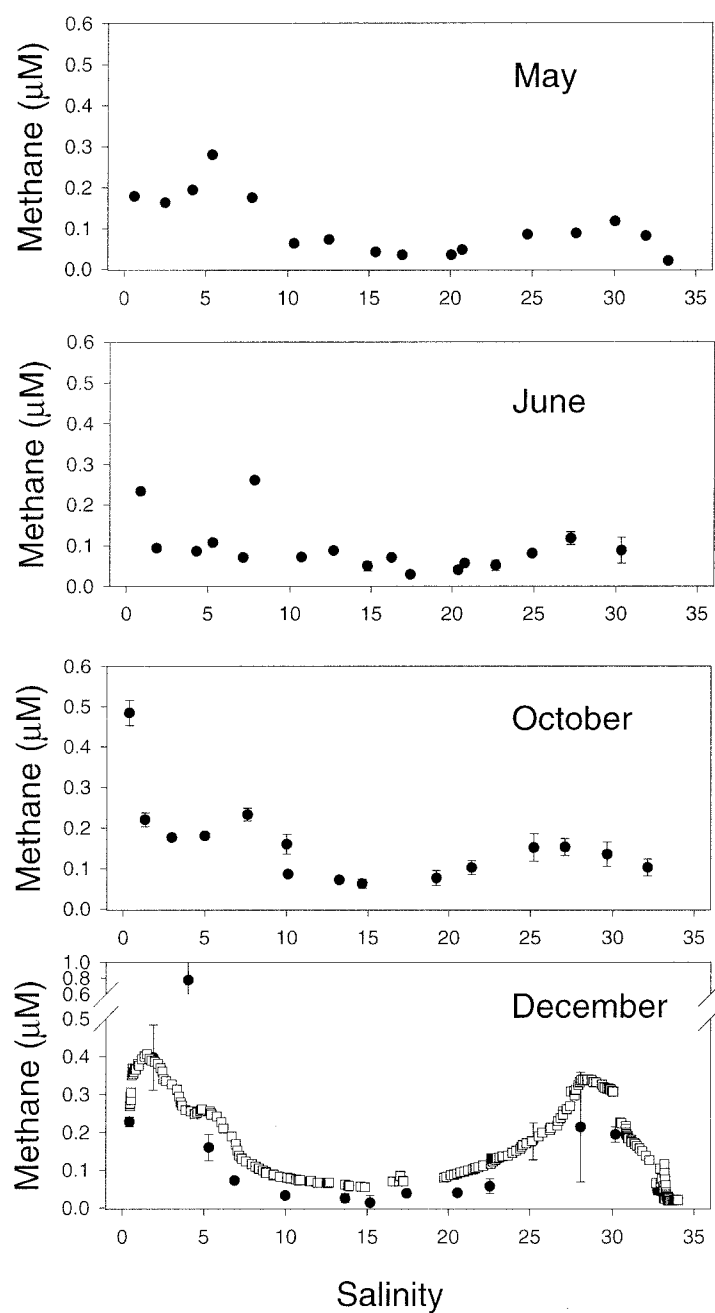
Figure 5. Dissolved methane versus salinity in the Scheldt estuary. Solid symbols: average ± standard deviation of discrete samples; Open squares: equilibrator-IR data. Notice the difference and break in methane concentration scale for December 1996.
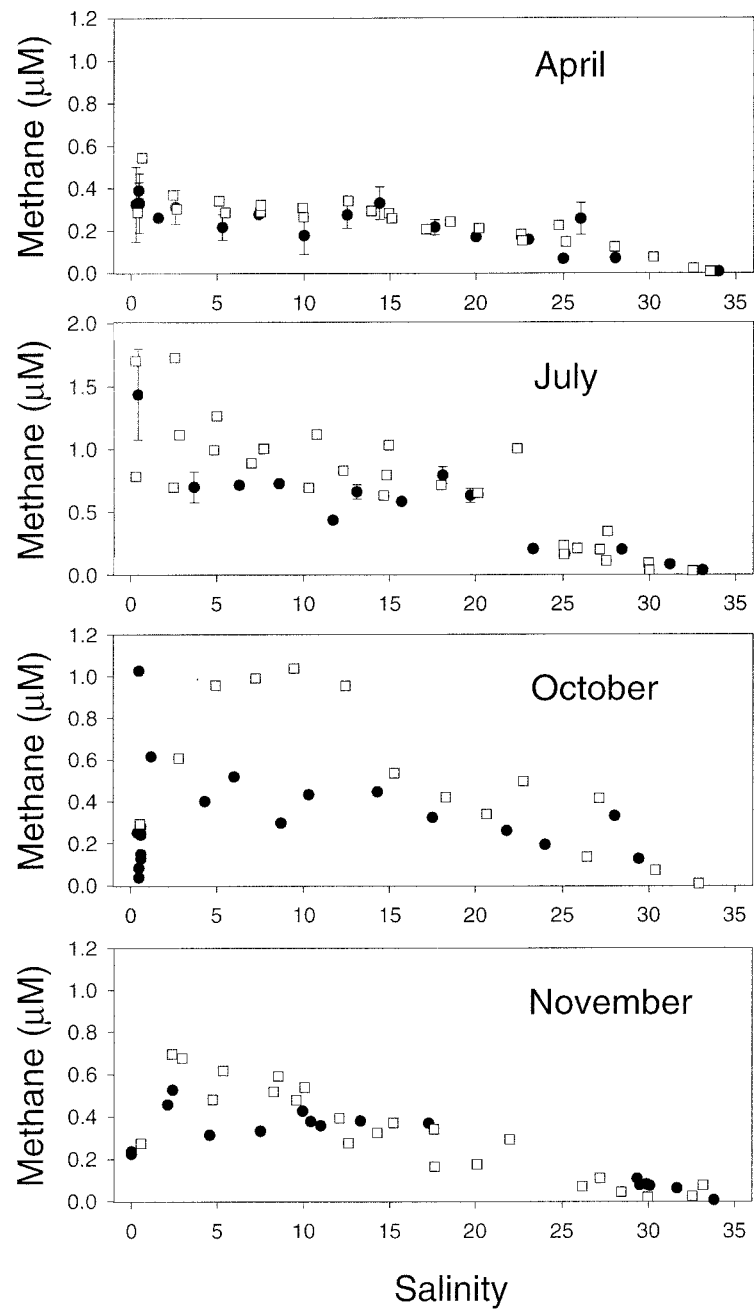
Figure 6. Dissolved methane versus salinity in the Rhine estuary. Solid symbols: average ± standard deviation of discrete samples; Open squares: equilibrator-GC-FID data. Notice the difference in methane concentration scale for July 1997.

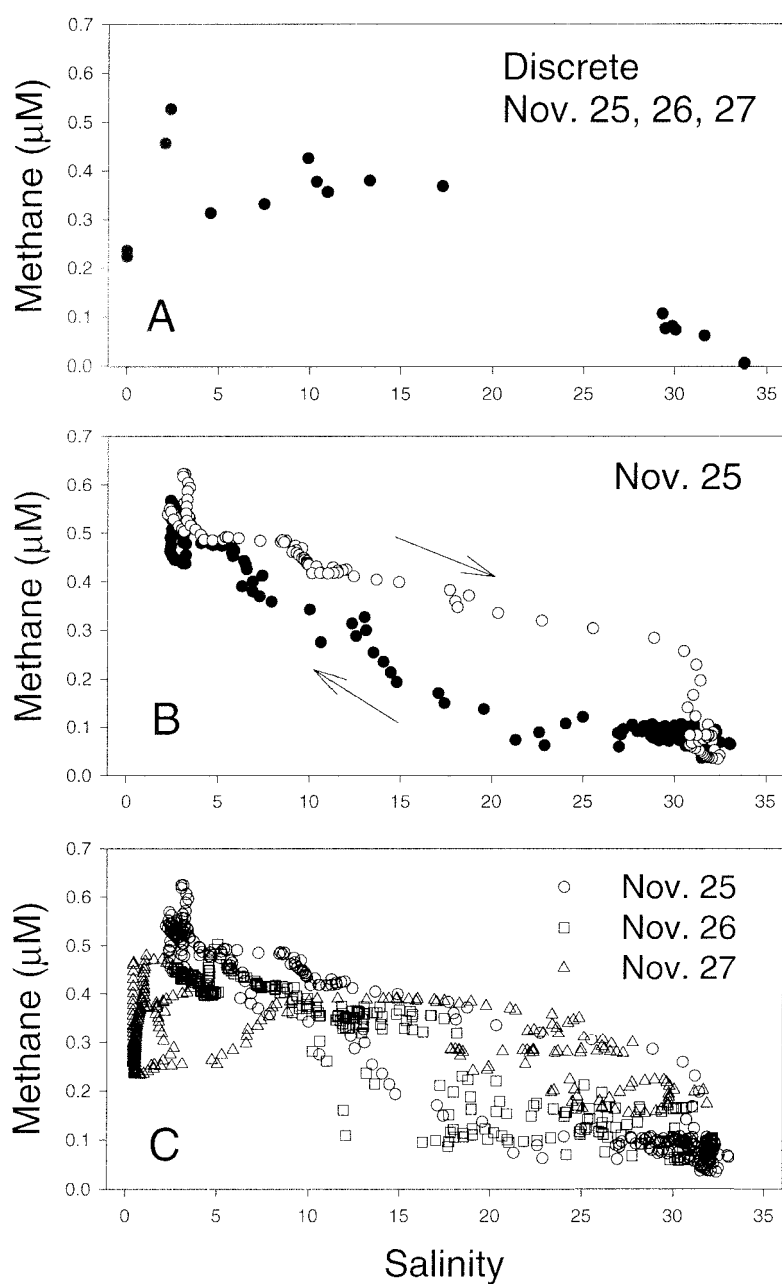*Figure 7.* Dissolved methane versus salinity in the Rhine estuary. A: Discrete samples collected during November 25, 26 and 27, 1997. B: Continuous on-line monitoring by equilibrator-IR method on November 25, 1997. Data collected sailing upstream (solid dots) and downstream (open dots) have been indicated. C: Continuous on-line monitoring by equilibrator-photo-acoustic-IR method during November 25, 26 and 27, 1997.
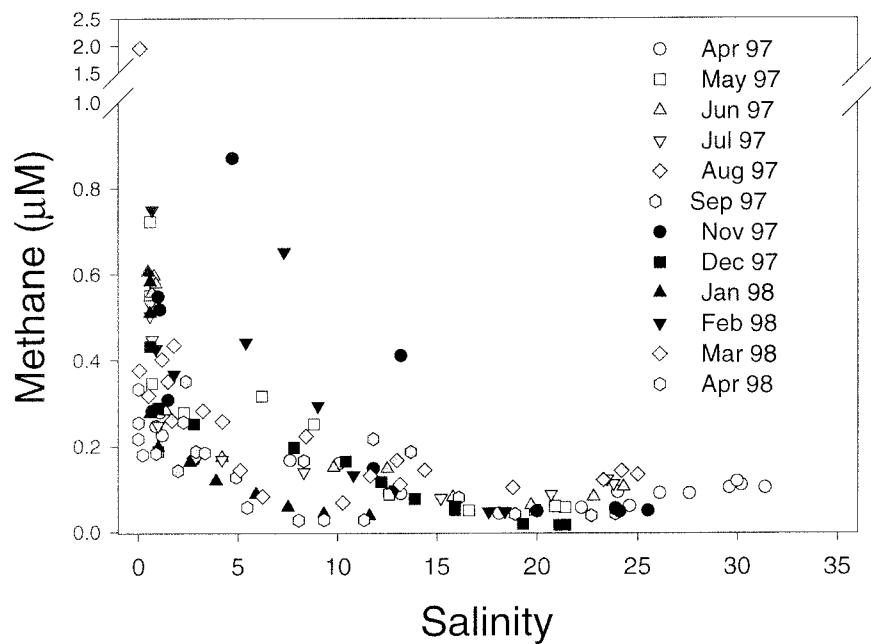
Figure 8. Dissolved methane versus salinity in the Scheldt estuary during April 1997 to April 1998 based on one-day cruises and equilibrator-photo-acoustic-IR method.

Figure 7 compares the distribution of methane in the Rhine estuary based on discrete samples collected during November 25, 26 and 27 with that based on equilibrator-IR data collected on November 25 only and that based on pooling equilibrator-IR data of November 25, 26 and 27. The methane-salinity relationships based on discrete and on-line equilibrator sampling are largely consistent (compare Figure 7(A) and 7(C)), but the relationship is highly variable (Figure 7(B)). Measurements of carbon dioxide and nitrous oxide collected simultaneously showed smooth, reproducible property versus salinity relationships (data not shown), indicating that this variability is unique to methane.

The Gironde, Scheldt and Rhine estuaries have been investigated four times to study seasonal variability (Figures 4–6). In the Rhine estuary there was clear seasonality with concentrations being high in summer and autumn and relatively low in winter and early spring. Seasonality in the Scheldt and Gironde estuaries was rather limited. Figure 8 shows the monthly variability of dissolved methane in the upper Scheldt estuary obtained using the equilibrator-IR technique during one-day cruises. This detailed time series supports the results shown in Figure 5, including the methane spikes at salinities near 5.

Table 3. Summary of saturation ratios and concentration gradients (relative to an atmospheric mixing ratio of 1.9 ppmv)

Cruise	N	Saturation ratio		Concentration gradient (nmol dm^{-3})	
		Range	Median	Range	Median
Elbe	20	1.3–29.8	5.8	0.9–108	17
Ems	13	9.2–131	31.5	24–372	86
Thames	15	1.5–67	5.7	1.7–269	17
Rhine	69	1.4–497	84	1.2–1430	273
Apr. 98	18	1.4–113	78.6	1.2–386	255
July 97	14	12.4–497	225	29–1430	600
Oct. 96	20	11.5–323	91.5	34–1020	268
Nov. 97	17	1.4–141	84.4	1.3–523	310
Scheldt	63	3.8–204	32.1	10–771	86
May 98	16	7.5–97	31.6	17–278	81
Jun. 96	17	10.6–93	29.9	26–258	78
Oct. 98	15	21–148	53.1	60–481	149
Dec. 96	15	3.8–204	19.4	10–771	69
Loire	16	3.4–231	6.6	7–668	14
Gironde	68	0.7–134	5.8	−0.9–526	13
Feb. 98	16	1.4–134	3.2	1.6–526	7.2
Jun. 97	14	2.9–53.4	5.9	5.3–140	13
Sep. 97	19	3.2–112	8.1	5.7–268	19
Oct. 96	19	0.7–95	5.1	−0.9–298	13
Douro	13	6.2–57.2	36.1	13–160	94
Sado	15	9.4–1580	59	19–3570	125
All	292	0.7–1580	24.9	−0.9–3570	68.2

Discussion

Dissolved methane concentrations in rivers, estuaries and coastal environments are highly variable at various spatial and temporal scales (Figures 3 to 6; De Angelis & Lilley 1987; De Angelis & Scranton 1993; Watanabe et al. 1994; Bange et al. 1998; Jones & Mulholland 1998a). A large database should consequently be constructed to cover this variability and to understand the factors governing dissolved methane concentrations and methane emission from estuarine environments. One basic requirement of such a database should be the internal consistency of the data. Our study shows that consistent

Table 4. Summary of fresh-water and marine end-members

Cruise	Freshwater end-member (nM)		Marine end-member (nM)	
	Salinity	Concentration	Salinity	Concentration
Elbe	0.4	111	29.1–29.3	4.2–5.9
Ems	0.7	51	29.8	91
Thames	0.4	273	33.8	5.0
Rhine				
Apr. 98	0.0–0.4	324–390	32.5	4.2
July 97	0.4	1437	33.1	31
Oct. 96	0.0–0.4	37–1026	29.4	125
Nov. 97	0.1	224	33.8	4.1
Scheldt				
May 98	0.6	179	33.3	20
Jun. 96	0.9	234	30.3	89
Oct. 98	0.4	485	32.1	103
Dec. 96	0.4	228	32.8	47
Loire	0–0.4	10–671	33.3	15.6
Gironde				
Feb. 98	0–0.2	90–559	35.1	3.7
Jun. 97	0–0.2	21–121	29.4	10.9
Sep. 97	0–0.1	10–55	30.8	15
Oct. 96	0	76–300	29.5	7.9
Douro	0–0.1	63–128	30.0	15
Sado	3.4	40	35.8	37

data can be obtained using different sampling methodologies (discrete, continuous), partitioning approaches (static headspace, purge-trapping and equilibrators) and methane detection techniques (GC-FID, photo-acoustic-IR). The consistency of samples measured directly and after storage (Figure 2(A)) indicates that rivers and estuaries in remote areas can be studied with limited logistic requirements. The photo-acoustic-IR analyser has been designed for on-line monitoring during extensive periods without human intervention or calibration. Coupling of this automatic monitoring device with an equilibrator offers the possibility for high-resolution studies of dissolved methane (and nitrous oxide and carbon dioxide) with minimal effort.

Dissolved methane in the fresh-water end-members varied from 0.01 to 1.4 μM (Table 4), consistent with literature data on methane in rivers that range from 0.005 to 8 μM (Table 5). A direct comparison with the rivers

Table 5. Concentrations of methane in rivers (and some upper estuaries)

River	Concentration (μM)	Reference
Mississippi River	0.10–0.37	Swinnerton & Lamontagne 1974
York River, Virginia	0.03–0.04	Lamontagne et al. 1973
Potomac River, DC, USA	1.7	Lamontagne et al. 1973
Sepik River, New Guinea	0.08–0.13	Wilkinson et al. 1978
Coast Range rivers, Oregon	0.02–1.7	De Angelis & Lilley 1987
Cascade Range rivers, Oregon	0.005–0.08	De Angelis & Lilley 1987
Willamette Valley rivers	0.5–1.1	De Angelis & Lilley 1987
Amazon River	0.053 ± 0.091	Richey et al. 1988
Saale River, Germany	0.33–0.56	Berger & Heyer 1989
Hudson River	0.05–0.94	De Angelis & Scranton 1993
Upper Scheldt estuary	0.4–0.6	Scranton & McShane 1991
Elbe River	0.06–0.12	Wernecke et al. 1994
Rivers of the Pantanal wetland of Brazil	0.03–8	Hamilton et al. 1995
Rivers in Florida	0.04–0.69	Bugna et al. 1996
creeks near Tomales Bay, California	0.14–0.95	Sansone et al. 1998
Upper Elbe estuary	0.111	Rehder et al. 1998
Kaneohe stream, Hawaii	0.033	Sansone et al. 1999
Rivers in the Great Bay area, NH	0.58–2.44	Sansone et al. 1999

and estuaries investigated in this study is limited to the Elbe and Scheldt. Wernecke et al. (1994) have reported methane concentrations of 0.06 to 0.12 μM for the river Elbe, consistent with our observations. Rehder et al. (1998) presented a transect of methane in the Elbe estuary that was made during May 1994. Although their extrapolated river end-member concentration of 0.08 μM is in accordance with our observation in April 1997 (0.111 μM), they obtained a near linear relation between salinity and methane. For the upper Scheldt estuary (salinities 1 to 5), Scranton and McShane (1991) reported methane concentrations of 0.4 to 0.6 μM during winter 1990, consistent with data presented in Figures 5 and 8. De Wilde and Duyzer (1995) have reported a methane concentration transect for the Scheldt estuary during October 1993 that meets our observations in terms of concentration levels and shape of the profile.

Our data on upper estuaries and fresh-water end-members (Table 4) and those reported in the literature (Table 5) clearly document the variability of dissolved methane in rivers and the head of estuaries. Obligate anaerobic bacteria biologically generate methane; hence production is confined to anoxic environments. Richey et al. (1988) have reported correlations between oxygen depletions (as expressed in apparent oxygen utilisation) and

methane concentrations for tributaries of the Amazon, but not for the mainstream. Similarly, our data do not show a relation between dissolved oxygen and methane concentrations with well-oxygenated water of the Rhine being methane rich and oxygen depleted waters from the Loire having low methane concentrations.

Jones and Mulholland (1998a) have reported that riverine methane concentrations increase with increasing river size due to increases of groundwater seeps downriver. Groundwater can be extremely rich in methane (Bugna et al. 1998; Jones & Mulholland 1998b). River size may be an important factor governing methane concentrations in a single drainage basin (De Angelis & Lilley 1987), but is not the only important factor across different systems. Riverine end-members in small drainage basins such as those of the Ems (50 nM) and Sado (40 nM) are indeed relatively low, but those in the Thames (273 nM) and Scheldt (179 to 485 nM) are intermediate to high. Rivers having a large drainage basin such as the Elbe (111 nM) and Douro (63–128 nM) have low to intermediate concentrations, whereas the Loire and Rhine revealed variable and high concentrations (Table 4). Although process measurements, other gases and basic biogeochemical parameters (see Frankignoulle & Middelburg 2002, for an overview) complement our data on dissolved methane, we have not been able to identify relationships across the various riverine systems.

The distribution of dissolved methane in the two stratified estuaries (Douro and Rhine) appears rather scattered (Figures 3(E), 6 and 7). Part of this variability may be due to our sampling strategy, which was based (for reason of consistency with the other estuaries) on the assumption of a vertically and laterally well mixed water column. This scatter complicates clear identification of the spatial distribution of sources and sinks. Moreover, the Rhine with its high discharge creates a very large region of freshwater influence in the North Sea, which typically extends along the Dutch coast north-eastward and 30 km offshore (De Ruijter et al. 1997). The estuarine plume area is strongly confined in the methane vs. salinity plots and the sharp methane gradient at high salinities (Figure 7) is due to passing a distinct front between the North Sea proper and the plume. In the Rhine estuary interactions between river discharge and tides results in pulses of low salinity being transferred to the North Sea at tidal frequency (De Ruijter et al. 1997). These pulses may differ in methane concentration and contribute to the observed scatter (Figures 6 and 7).

Sansone et al. (1999) have used methane concentration and stable isotope data ($\delta^{13}CH_4$) in various estuarine systems and clearly identified and documented a number of estuarine sinks and sources. Consistently, the distribution of dissolved methane in the well-mixed estuaries clearly reflects the impor-

tance of estuarine sinks and sources. Dissolved methane concentrations initially decrease with increasing salinities (Elbe, Thames, Loire, Gironde, and Scheldt), then increase to a maximum (Ems, Sado, Gironde, and Scheldt) at intermediate to high salinities, before decreasing again offshore. The initial decrease of dissolved methane with increasing salinity is due to a high river end-member concentration and subsequent consumption of methane by oxidation and/or loss to the atmosphere. Methane oxidation can turnover the dissolved methane pool rapidly: 1.4 to 9 days in the upper Hudson estuary (De Angelis & Scranton 1993), <2 hour to 1 day in the Ogeechee River depending on temperature (Pulliam 1993). Van der Nat et al. (1997) reported methane oxidation rates for the surface layer of intertidal sediments from the upper Scheldt estuary corresponding to a turnover rate of about 2 hour. Clearly, methane oxidation is an important sink of methane in estuaries, but it strongly depends on the temperature (Pulliam 1993) and salinity with very low oxidation rates at salinities above 6 (De Angelis & Scranton 1993). During the BIOGEST campaigns methane outgassing and oxidation have been measured for a number of estuaries and the residence time for methane varied from 12 to 48 hours (Iversen, unpublished data).

The sources of methane at intermediate to high salinities likely include intertidal flats and marshes as indicated by the observation that estuaries showing the most pronounced maxima in dissolved methane (Ems, Sado and Scheldt) have extensive areas of intertidal sediments in their lower parts (Table 1). In addition, samples collected in tidal creeks (Figure 3(B) and 3(F)) and above tidal flat areas (Figure 4 September) have high methane concentrations and intertidal sediments have been reported as an important depocenter of organic matter and as a source of methane (Kelley et al. 1995; Middelburg et al. 1996; van der Nat & Middelburg 2000).

While the nature of the source of methane to estuaries may not have been resolved in this manuscript, it is clear from our study that estuaries represent a source of methane to the atmosphere. All samples, but one in the Gironde estuary, were above atmospheric equilibrium and saturation ratios varied between 0.7 to 1580 (Table 3). Our range of saturation values for methane in estuaries comprises that compiled by Bange et al. (1994), ranging from 1 to 1290 with an average of 12.3. Methane emission is proportional to the air-water concentration gradient (the driving force) and the air-water exchange coefficient (Liss & Merlivat 1986). Concentration gradients range from -0.9 to >3500 nmol dm^{-3} with the median value of the overall dataset being 68.2 nmol dm^{-3} (Table 3). Air-water exchange coefficients are a function of water surface agitation, which in turn is determined by turbulence (Liss & Merlivat 1986). In offshore areas most turbulence in surface waters is driven by wind and air-sea exchange coefficients (K) have been parameter-

ised as a function of wind (for a recent review see Frost & Upstill-Goddard 1999). In most rivers, turbulence due to interactions between stream and bottom topography is more important than wind stress in determining water surface conditions, partly because of wind protection. Air-water exchange coefficients in rivers are often parameterised as a function of stream velocity (Lilley et al. 1996; Marino & Howarth 1993). The factors determining air-water exchange in estuaries are more complex and likely change along the estuary from primarily stream current driven exchange in the upper estuary to wind driven exchange in the mouth. Moreover, most of the turbulence in tidal estuaries is due to tidal currents and their interaction with wind and bottom topography and clearly depends on the tidal energy and depth and morphology of the estuary. Most researchers have applied a wind speed based parameterisation to air-gas exchange to the estuarine reach and a current velocity based parameterisation to the river end-member (e.g. De Angelis & Lilley 1987), whereas some others have applied tracer or floating dome technique to actual measure exchange rates. Marino and Howarth (1993) have combined a floating dome technique and oxygen measurements to estimate air-sea exchange in the Hudson estuary. Water-air exchange coefficients ranged from 3 to 24.6 cm h^{-1}. Frankignoulle et al. (1996) have applied a floating dome technique to measure carbon dioxide exchange and obtained an exchange coefficients of 8.4 ± 3.1 cm h^{-1} for the Scheldt estuary during March 1993. Exchange coefficients based on carbon dioxide and the floating chamber technique determined during the BIOGEST cruises were 8 cm h^{-1} and higher (Frankignoulle et al. 1998 and personal communication).

On the basis of our median air-water concentration gradients (68.2 nmol dm^{-3}) and a conservative exchange coefficient of 8 cm h^{-1}, the minimum flux of methane from estuaries is about 0.13 mmol m^{-2} d^{-1}. This corresponds to a minimum global methane emission of 1.1 Tg CH_4 yr^{-1} (based on a global estuarine surface area of 1400 × 10^3 km^2). Bange et al. (1994) have applied global exchange coefficients to estimate the global methane emission by estuaries. Following their approach and surface areas, we estimate that estuaries emit 1.8 and 3.0 Tg CH_4 yr^{-1} for global area weighted transfer coefficients of 13.3 and 22.3 cm h^{-1}, respectively (Bange et al. 1994). Our estimates are somewhat higher than estimates (0.8 and 1.3 Tg CH_4 yr^{-1}) by Bange et al. (1994), because our degrees of saturation are higher. Nevertheless, this slightly upward revised emission estimate still represents <9% of the total oceanic emission (Bange et al. 1994), which in turn is a very small component of the global methane emission (Cicerone & Oremland 1988).

Acknowledgements

References

Amouroux D, Roberts G, Rapsomanikis S & Andreae MO (2002) Biogenic gas (CH_4, N_2O, DMS) emission to the atmosphere from nearshore and shelfwaters of the northwestern Black Sea. Est. Coast. Shelf Sci. (in press)

Abril G, Etcheber H, Le Hir P, Bassoullet P, Boutier B & Frankignoulle M (1999) Oxic/anoxic oscillations and organic carbon mineralisation in an estuarine maximum turbidity zone (The Gironde, France). Limnol. Oceanogr. 44: 1304–1315

Abril G, Riou SA, Etcheber H, Frankignoulle M, de Wit R & Middelburg JJ (2000) Transient, tidal time-scale nitrogen transformation in an estuarine turbidity maximum-fluid mud system (The Gironde, S.W. France). Est. Coast. Shelf Sci. 50: 703–715

Bange HW, Bartell UH, Rapsomanikis S & Andreae MO (1994) Methane in the Baltic and North Seas and a reassessment of the marine emissions of methane. Global Biogeoch. Cycles 8: 465–480

Bange HW, Rapsomanikis S & Andreae MO (1996) The Aegaen Sea as a source of atmospheric nitrous oxide and methane. Marine Chemistry 53: 41–49

Bange HW, Dahlke S, Ramesh R, Meyer-Reil LA & Andreae MO (1998) Seasonal study of methane and nitrous oxide in the coastal waters of the southern Baltic Sea. Est. Coast. Shelf Sci. 47: 807–817

Berger U & Heyer J (1989) Untersuchungen zum Methankreislauf in der Saale. J. Basic Microb. 29: 195–213

Bugna GC, Chanton JP, Cable JE, Burnett WC & Cable PH (1996) The importance of groundwater discharge to the methane budgets of nearshore and continental shelf waters of the Gulf of New Mexico. Geochim. Cosmochim. Acta 60: 4735–4746

Cicerone RJ & Oremland RS (1988) Biogeochemical aspects of atmospheric methane. Global Biogeoch. Cycles 2: 299–327

De Angelis MA & Lilley MD (1987) Methane in surface waters of Oregon estuaries and rivers. Limnol. Oceanogr. 32: 716–722

De Angelis MA & Scranton MI (1993) Fate of methane in the Hudson River and estuary. Glob. Biogeoch. Cycles 7: 509–523

De Angelis MA & Lee C (1994) Methane production during zooplankton grazing on marine phytoplankton. Limnol. Oceanogr. 39: 1298–1308

De Ruijter WPM, Visser AW & Bos WG (1997) The Rhine outlow: A prototypical pulsed discharge plume in a high energy shallow sea. J. Mar. Syst. 12: 263–276

De Wilde HPJ & Duyzer JH (1995) Methane emission off the Dutch coast: air-sea concentration differences versus atmospheric gradients. In: Jähne B & Monahan E (Eds) Air-Sea Gas Transfer (pp 763–773). AEON Verlag, Hanau Germany

De Wilde HPJ & Helder W (1997) Nitrous oxide in the Somali Basin: The role of upwelling. Deep Sea Res. II, 44: 1319–1340

Frankignoulle M, Bourge I & Wollast R. (1996) Atmospheric CO_2 fluxes in a highly polluted estuary (the Scheldt). Limnol. Oceanogr. 41: 365–369

Frankignoulle M, Abril G, Borges A, Bourge I, Canon C, Delille B, Libert E & Théate J-M (1998) Carbon dioxide emission from European estuaries. Science 282: 434–436

Frankignoulle M & Middelburg JJ (2002) Biogases in tidal European Estuaries: the BIOGEST project. Biogeochem. 59: 1–4

Frost T & Upstill-Goddard RC (1999) Air-sea exchange into the millennium: Progress and uncertainties. Ocean. Mar. Biol. Ann. Rev. 37: 1–45

Hamilton SK, Sippel SJ & Melack JM (1995) Oxygen depletion and carbon dioxide and methane production in waters of the Pantanal wetland of Brazil. Biogeochem. 30: 115–141

Hovland M, Judd AG & Burke RA (1993) The global flux of methane from shallow submarine sediments. Chemosphere 26: 559–578

Jones RD & Amador JA (1993) Methane and carbon monoxide production, oxidation and turnover times in the Caribbean Sea as influenced by the Orinoco river. J. Geophys. Res. 98: 2353–2359

Jones JB & Mulholland PJ (1998a) Influence of drainage basin topography and elevation on carbon dioxide and methane supersaturation of stream water. Biogeochemistry 40: 57–72

Jones JB & Mulholland PJ (1998b) Methane input and evasion in a hardwood forest stream: Effects of subsurface flow from shallow and deep pathways. Limnol. Oceanogr. 43: 1243–1250

Kelley CA, Martens CS & Ussler III W (1995) Methane dynamics across a tidally flooded riverbank margin. Limnol. Oceanogr. 40: 1112–1129

Lamontagne RA, Swinnerton JW, Linnenbom VJ & Smith WD (1973) Methane concentrations in various marine environments. J. Geoph. Res. 78: 5317–5323

Lilley MD, de Angelis MA & Olson JE (1996) Methane concentrations and estimated fluxes from Pacific Northwest rivers. Mitt. Internat. Verein. Limnol. 25: 187–196

Liss PS & Merlivat L (1986) Air-Sea exchange rates: Introduction and synthesis. In: Buat-Menard P (Ed) The Role of Air-Sea Exchange in Geochemical Cycling (pp 113–127). D. Reidel Publishing Company, Dordrecht

Marino R & Howarth RW (1993) Atmospheric oxygen exchange in the Hudson River: dome measurements and comparison with other natural waters. Estuaries 16: 433–445

Michaelis W, Boenisch G, Jennisch A, Ladage S, Richnow HH, Seifert R & Stoffers P (1990) Methane and ^{3}He anomalies related to submarine intraplate volcanic activities. Mitt. Geol. Pal. Inst. Univ. Hamburg 69: 117–127

Middelburg JJ, Klaver G, Nieuwenhuize J, Wielemaker A, de Haas W & van der Nat JFWA (1996) Organic matter mineralization in intertidal sediments along an estuarine gradient. Mar. Ecol. Prog. Ser. 132: 157–168

Prather M, Derwent R, Ehhalt D, Fraser P, Sanhueza E & Zhou X. (1995) Other trace gases and atmospheric chemistry. In: Houghton JT et al. (Eds) Climate Change 1994. Radiative Forcing of Climate Change and an Evaluation of the IPCC IS92 Emission Scenarios (pp 73–126). Cambridge University Press, Cambridge

Pulliam WM (1993) Carbon dioxide and methane exports from a southeastern floodplain swamp. Ecol. Monogr. 63: 29–53

Rehder G, Keir RS, Suess E & Pohlmann T (1998) The multiple sources and patterns of methane in North Sea waters. Aquat. Geochem. 4: 403–427

Richey JE, Devol AH, Wofsy, SC, Victoria R & Riberio MNG (1988) Biogenic gases and the oxidation and reduction of carbon in Amazon River and floodplain waters. Limnol. Oceanogr. 33: 551–561

Sansone FJ, Rust TR & Smith SV (1998) Methane distribution and cycling in Tomales Bay. Estuaries 21: 66–77

Sansone FJ, Holmes ME & Popp BN (1999) Methane stable isotopic ratios and concentrations as indicators of methane dynamics in estuaries. Glob. Biogeoch. Cycles 13: 463–474

Scranton MI & McShane K (1991) Methane fluxes in the southern North Sea: the role of European rivers. Cont. Shelf Res. 11: 37–52

Seifert R, Delling N, Richnow HH, Kempe S, Hefter J & Michaelis W (1999) Ethylene and methane in the upper water column of the subtropical Atlantic. Biogeochemistry 44: 73–91

Swinnerton JW & Lamontagne RA (1974) Oceanic distribution of low-molecular-weight hydrocarbons: Baseline measurements. Environ. Sci. Tech. 8: 657–663

Van der Nat JFWA de Brouwer JFC, Middelburg JJ & Laanbroek HJ (1997) Spatial distribution and inhibition by ammonium of methane oxidation in intertidal freshwater marshes. Appl Environ. Microb. 63: 4734–4740

Van der Nat JFWA & Middelburg JJ (2000) Methane emission from tidal freshwater marshes. Biogeochem. 49: 103–121

Watanabe S, Higashitani N, Tusurshima N & Tsunogai S (1994) Annual variation of methane in seawater in Funka Bay, Japan. J. Oceanogr. 5: 415–421

Wernecke G, Flöser G, Korn S, Weitkamp C & Michaelis W (1994) First measurements of the methane concentration in the North Sea with a new in-situ device. Bull. Geol. Soc. Denmark 41: 5–11

Wiesenburg DA & Guinasso NLJ (1979) Equilibrium solubilities of methane, carbon monoxide, and hydrogen in water and seawater. J. Chem. Eng. Data 24: 356–360

Wilkniss PE, Lamontagne RE, Larson RE & Swinnerton JW (1978) Atmospheric trace gases and land and sea breezes at the Sepik River Coast of Papua, New Guinea. J. Geophys. Res. 83: 3672–3574